Scanning Nanocalorimetry at High Cooling Rate of Isotactic Polypropylene

Felice De Santis,*,† Sergey Adamovsky,‡ Giuseppe Titomanlio,† and Christoph Schick‡

Department of Chemical and Food Engineering, University of Salerno, 84084 Fisciano (SA), Italy, and Institute of Physics, University of Rostock, 18051 Rostock, Germany

Received November 25, 2005; Revised Manuscript Received February 7, 2006

ABSTRACT: A wide set of cooling scans and subsequent melting behavior of isotactic polypropylene (i-PP) were investigated using differential scanning calorimetry and nanocalorimetry at very high cooling rate. The latter technique offers, indeed, the distinctive possibility to perform heat capacity measurements at rates of more than 1000 K/s, both in cooling and in heating, to characterize the crystallization. When the i-PP sample was solidified with cooling rate larger than 160 K/s, a novel enthalpic process was observed that was related to the mesomorphic phase formation. Furthermore, at cooling rates higher than 1000 K/s, the i-PP sample did not crystallize neither in the α nor in the mesomorphic form. The subsequent heating scan starting from −15 °C showed an exothermic event, between 0 and 30 °C, ascribed to the mesophase cold crystallization.

Introduction

Isotactic polypropylene (i-PP) is one of the most investigated polymers because of its commercial and industrial importance. Depending on thermal treatments, molecular mass, and degree of tacticity, when crystallized from the melt, the i-PP chains can organize several spatial arrangements giving rise to three different crystalline polymorphs: α-monoclinic, β-hexagonal, and γ-triclinic.[1−3] Moreover, when i-PP is quenched from the melt to low temperature, for example in an ice bath at 0 °C, a biphasic system is obtained: one phase is amorphous, the other has an order intermediate between the amorphous and the crystalline phase, denoted with different names in the literature: smectic,[4] paracrystal,[5] glass,[6] or mesomorphic phase.[7] The mesomorphic phase is stable at room temperature for long periods, but it transforms into the α-monoclinic form when heated, for example, above 60 °C.[8]

Several studies, which have been carried out on the subject of crystallization of α-phase of i-PP, include the morphology of the single crystals,[9−11] the Avrami analysis of the isothermal crystallization process,[12,13] and the kinetics of the growth rates.[14,15] The classical picture of quiescent polymer crystallization involves, first, the creation of a stable nucleus from the entangled polymer melt and, second, the growth of crystalline lamellar structures which remain included into quasi-spherical entities, spherulites, made of both amorphous and crystalline phases.

Phase distribution of i-PP samples, after quenching over a wide range of cooling rates, was estimated by a deconvolution procedure applied to WAXS spectra by Piccarolo et al.[16] To investigate the effect of the cooling rate on crystallization, thin films were quenched and cooling thermal histories were carefully monitored. The cooling rate evaluated at 70 °C was identified for i-PP as representative of a particular cooling history.[17] At cooling rates lower than 10−20 K/s only the spherulitic α-monoclinic phase was observed in the solidified film; above 200 K/s, only the mesomorphic phase was found;[17] between 20 and 200 K/s, both α-monoclinic and mesomorphic phases were detected by WAXS analysis of the solid samples, the latter prevailing at higher cooling rates.

Although the fact that the mesomorphic phase develops during crystallization from molten i-PP at cooling rates higher than 20 K/s is known, the mechanism, the temperature range, and the kinetics of formation of the smectic phase are still debated; several hypotheses, for instance, have been proposed to explain the mechanism of initial stages of crystallization from the polymer melt.[18−21] Furthermore, only recently kinetics of formation of the mesophase was considered in a crystallization kinetics model describing calorimetric results and both morphology and phase distribution in samples characterized after the solidification.[14]

The analysis of quenched samples, however, does not reveal when the crystallization process toward mesomorphic phase takes place; neither this can be monitored by conventional calorimetry, which is used to study temperature-activated processes, like crystallization, during temperature scans at cooling rates up to 1−8 K/s,[22,23] as at these cooling rates the mesomorphic phase does not form. Preliminary results on i-PP crystallization at cooling rates up to 70 K/s were published by Wunderlich et al.[24] using a DTA technique.

Heating rate of calorimeters is generally limited by the total heat capacity (sample + addenda), the maximum power transferred to the system, and speed of temperature measurement.[25] Recently developed quasi-adiabatic nanocalorimeters can operate at very high heating rates[26−29] because of very small addenda and sample heat capacities. Cooling rate, which is not controlled for the quasi adiabatic systems, is limited by total heat capacity, sample size, and heat losses.[30,31] A thin film nanocalorimeter under nonadiabatic conditions allows cooling as well as heating rates of more than 10 000 K/s[30−32] and, thus, allows monitoring the crystallization of polymers in cooling ranges never explored earlier.[30,33−36]

In this paper, the crystallization under quiescent conditions from the melt and subsequent melting behavior of i-PP is thoroughly investigated using differential scanning calorimetry and nanocalorimetry at rates up to 1000 K/s.

† University of Salerno.
‡ University of Rostock.
* To whom correspondence should be addressed. E mail: fedesantis@unisa.it.

10.1021/ma052525n CCC: $33.50
Published on Web 03/10/2006

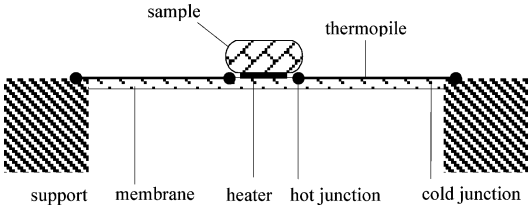

Figure 1. Scheme of the sensor.

Experimental Section

The i-PP grade adopted in this study was supplied by Montell, and its commercial name is T30G (nonnucleated, $M_w = 376\,000$, $M_w/M_n = 6.7$, tacticity = 87.6%). The crystallization of the same resin was object of several studies.[14,37−40] A detailed description of the apparatus adopted for the nanocalorimetry experiments is available elsewhere.[30,31,33,41] Only a schematic description is given below. The sensor, TCG-3880 of Xensor Integration NL,[42,43] consists of a thin SiN_x membrane (thickness ca. 500 nm, size 1 mm × 2 mm), located on a supporting frame.

A small heater (active area 50 μm × 100 μm) is placed in the center of the membrane to heat up the sample (see Figure 1). Around the heater there are the six "hot" junctions of a semiconducting thermopile, which is used to measure the sample's temperature during controlled and essentially linear heating and cooling at rates between 15 and 1000 K/s. The cold junctions are on the edge of the membrane on a relatively thick support; thus their temperature remains equal to the ambient temperature. The thermopile and the heater are connected via amplifiers to an ADC-DAC computer board so that the heater voltage can be controlled by the software and actual heater voltage and current as well as thermopile voltage can be recorded as a function of time.[33]

The sensor was placed inside a massive copper block connected to a cooling system (Lauda RC-6). The temperature was controlled by a Julabo MC-E″ temperature controller using a Pt100 platinum temperature sensor and a heater; the accessible temperature range was from −20 to 150 °C for the copper block. All measurements were carried out under a nitrogen atmosphere to prevent oxidative degradation of the sample.

From the heat balance, taking into account the power needed to heat sample and addenda at the given rate, heat losses to the surrounding as well as the electrical power applied to the heater, the total heat capacity can be obtained; for details see refs 30 and 41. Addenda heat capacity of the order of 150 nJ/K was not subtracted because the same sensor and the same sample were used for all experiments discussed here.[41] The uncertainty of the heat capacity measurement is about 20% while the reproducibility is much better (see Figure 7). Temperature calibration is affected by two serious problems: (i) thermopile sensitivity, which was determined from melting peaks of indium, tin, and lead at different cooper block temperatures; (ii) the distance between sample and thermopile hot junctions. The temperature profile around the heater was modeled, and the measured values were accordingly corrected.[31,41] It should be mentioned that even at rates of 1000 K/s the system could be described as quasi-static. Because of the small dimension (μm) thermal waves and resulting thermal lags are not important.[31] In total uncertainty in temperature is up to 10 K slightly depending on rate. Reproducibility of the temperature measurement is much better, as can be seen from Figure 7.

A small i-PP sample was cut from a pellet under a microscope and placed very carefully onto the center of the sensor membrane, as described in refs 30, 33, and 41. An electric current was then applied to the heater to melt the sample and to fix it on the membrane of the sensor. The sample of the order of 100 ng becomes a droplet of 60−80 μm diameter. All the measurements showed in this paper were performed with the same sample. Sample mass was not independently determined, and therefore the apparent heat capacity and not specific heat capacity is given in the figures below.

Nominal cooling rates were reached very fast. The cooling rate of 1000 K/s, as shown in Figure 2, was reached within less than

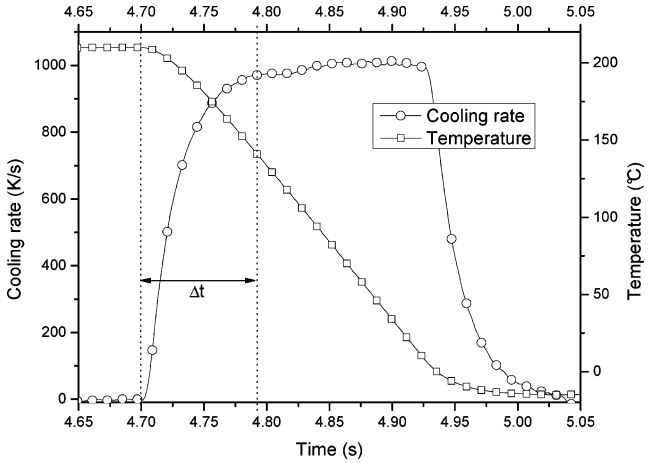

Figure 2. Experimental cooling rate and temperature vs time during cooling step at 1000 K/s.

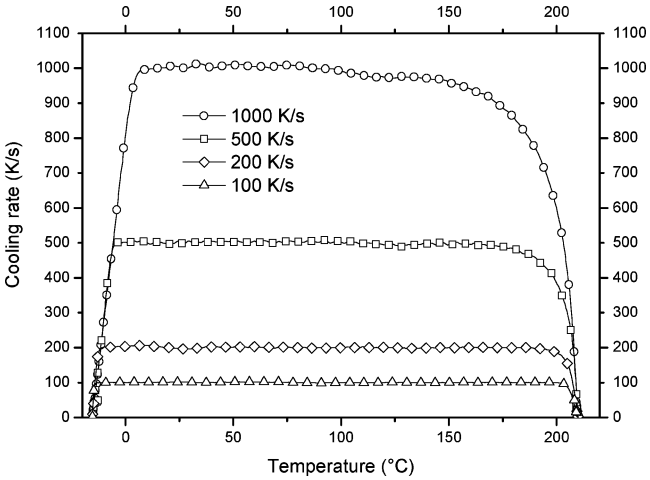

Figure 3. Cooling rate vs temperature; cooling runs (nominal cooling rate: 100, 200, 500, 1000 K/s) from 210 to −15 °C.

one tenth of a second, ensuring that the nominal cooling rate is already achieved around 150 °C, as shown in Figure 3, thus well before the crystallization process starts.

The cooling characteristic in the interval from 210 to −15 °C of the assembly sample sensor is reported in Figure 3, as cooling rate vs temperature. The cooling rate is limited by the sample size and by the cooling system. The final approach to the temperature of the copper block follows a common exponential decay, as seen below 0 °C in Figure 3.

Tests were performed adopting the experimental protocols schematically shown in Figure 4; in particular, the sample was heated at 50 K/s from −15 to 210 °C and held at this temperature for 0.1 s. The sample was then cooled to −15 °C with rates in the range 15−1000 K/s, and after cooling it was maintained at this temperature for 0.1 s. The minimum cooling rate was 15 K/s due to limits of the apparatus sensitivity. The sample, after being held 0.1 s at −15 °C, was heated again in the nanocalorimenter to 210 °C at 50 K/s. Reproducibility was recurrently tested, and differences in thermograms were not noticed even after ca. 200 experiments. Therefore, degradation was considered negligible, also because the sample was held at temperatures above the melting temperature for only about 0.2 s during each experiment.

Results and Discussion

Cooling Scans. After melting at 210 °C, the i-PP sample was investigated in the subsequent cooling scans in a wide range of cooling rates.

The thermograms of some selected cooling scans are shown in Figure 5 (the complete set of cooling scans and the 3D plot are reported in the Supporting Information).

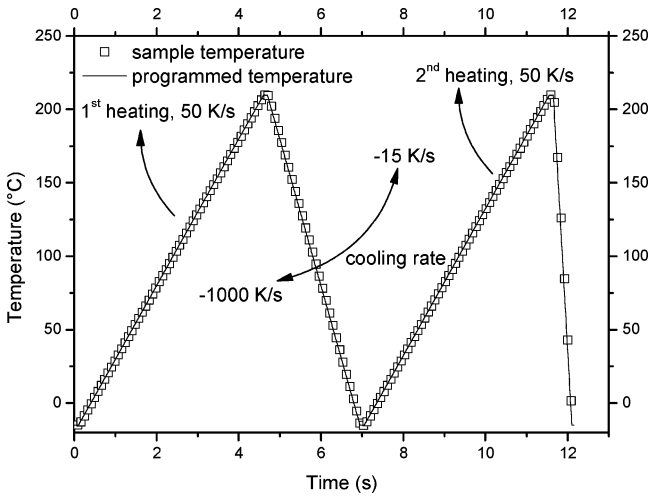

Figure 4. Experimental protocol, sample, and programmed temperature. During cooling runs the cooling rate was programmed to be 15 up to 1000 K/s.

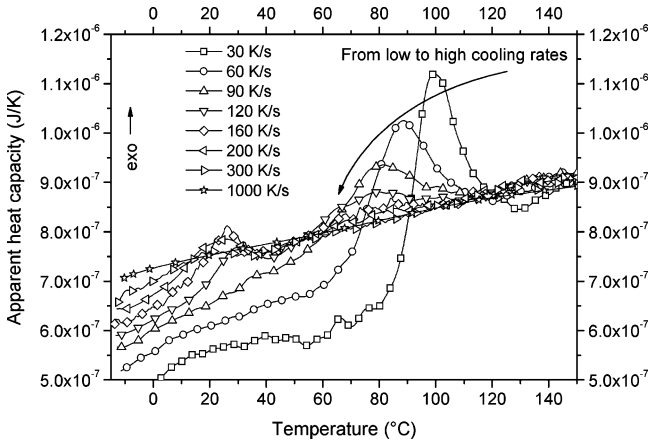

Figure 5. Thermograms of i-PP sample at selected cooling rates (30, 60, 90, 120, 160, 200, 300, and 1000 K/s).

For cooling rates up to about 90 K/s, only one well-defined exothermal peak is observed. This is in agreement with the analysis of samples solidified during either standard calorimetric or quenching tests, performed on the same i-PP grade,[14,44] which show that at low cooling rate only the α-monoclinic form is obtained during solidification. For a quantitative comparison between linear cooling and quenching experiments,[14,16] it has however to be considered that for the latter cooling rates decrease with decreasing temperature. For the quenching experiments cooling rates were determined at 70 °C whereas, as shown in Figure 5, crystallization of the α-phase starts already at about 120 °C. Consequently, cooling rates at 70 °C during quenching experiments have to be roughly doubled for a proper comparison with results of constant cooling rate. The exothermal peak, shown by the thermograms of the sample, which was cooled with cooling rates equal to or smaller than 90 K/s, can, thus, certainly be attributed to the melt-crystallization toward the crystalline α-monoclinic phase.

As expected, on increasing the cooling rate, a shift of the α crystallization peak to lower temperatures is observed. The temperature of the peak maximum decreases as cooling rate increases; in particular, it decreases from 107 to 76 °C for an increase of cooling rate from 15 to 160 K/s. The width of the crystallization peak remains about 60 K, whereas the peak height (and with it final α-crystallinity) decrease with increasing cooling rate.

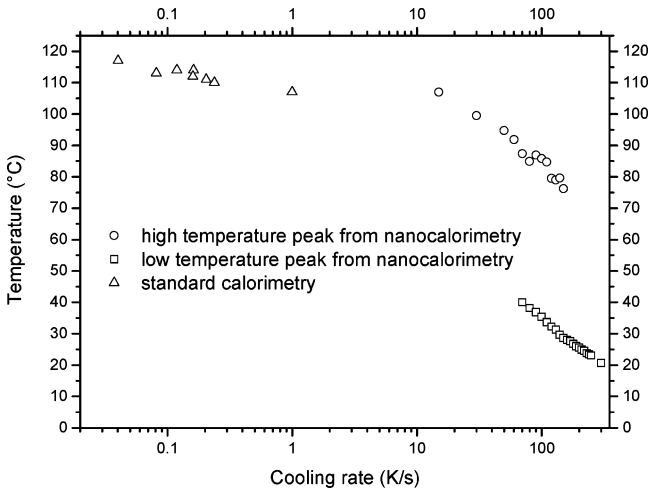

Figure 6. Exothermal peak position vs cooling rate from thermograms at different cooling rates: standard DSC (0.02−1 K/s), nanocalorimeter (15−300 K/s).

For cooling rates higher than about 90 K/s, a second exothermal peak appears at low temperatures. At cooling rate of 120 K/s this new exothermal event takes place between 43 and 12 °C (peak position at 29 °C), and the area of the new peak slowly increases up to a cooling rate of 160 K/s. At the cooling rates larger than 150 K/s, the first peak disappears and also the intensity of the second peak decreases on increasing cooling rate; a shift of this second exothermal peak to lower temperatures is also evident as cooling rate increases. Essentially mesomorphic samples were obtained by quenches[14,16] of i-PP to room temperature with cooling rates larger than 100 K/s at 70 °C. The low-temperature exothermal event, shown in Figure 5, can thus be ascribed to the mesophase formation. To our knowledge, this is the first time that the development of the i-PP mesophase is monitored during solidification from the melt.

Finally, at cooling rates higher than of 1000 K/s, both peaks are not visible in the heat capacity evolution with temperature, and the related thermogram appears as a straight line, as reported in Figure 5. The i-PP sample does not crystallize neither in the α-form nor in the mesomorphic form and remains amorphous at −15 °C, which is just below the glass transition temperature of the amorphous i-PP, at about −10 °C.

The final level of heat capacity, shown in Figure 5, increases on increasing the cooling rate. This is consistent with an increase of the amorphous content with increasing the cooling rate.

The peak temperatures of all the cooling experiments carried out with the nanocalorimeter apparatus are compared in Figure 6 with the peak temperatures detected by standard calorimetry on the same material. The trend of exothermal peaks is summarized, plotting the temperature peak position: the first one at high temperature attributed to the α-phase and the second at low temperature attributed to the mesophase, observed in the thermograms at different cooling rates.

The α-phase peak temperatures obtained from nanocalorimetry seem to be slightly higher than what is expected from a simple extrapolation of data obtained from standard DSC, but it is almost within the uncertainty in temperature. Although the comparison is between data at very different cooling rates and sample sizes, this may suggest that a relevant effect of the surface on nucleation density could be considered.

The mesophase formation is observed at low temperature. The temperature of the peak maximum decreases as cooling rate increases; in particular, it decreases from 40 to 20 °C for an increase of cooling rate from 70 to 300 K/s.

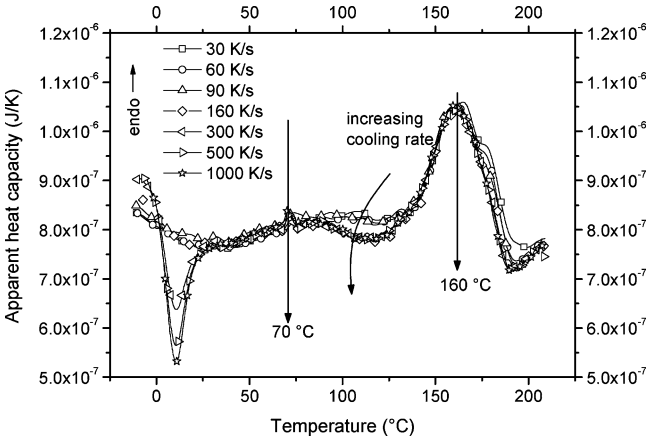

Figure 7. Selected thermograms of i-PP sample (solidified with cooling rates of 30, 60, 90, 160, 300, 500, and 1000 K/s) at a heating rate of 50 K/s.

Subsequent Heating Behaviors. The i-PP morphologies, resulting from the solidification described in the previous section, namely performed in a wide range of cooling rates, were investigated by subsequent heating at 50 K/s.

The thermograms of some selected scans performed at a heating rate of 50 K/s are also shown in Figure 7 (the complete series of heating scans and the 3D plot are reported in the Supporting Information).

The thermograms in Figure 7 are consistent with those reported in Figure 5. Indeed, only one well-defined endothermic peak at 160 °C is observed in the thermograms of the heating scans performed after solidification at cooling rates from 15 to 90 K/s, which had given rise to crystallization toward the α-monoclinic phase. That peak is obviously due to the melting of the α-monoclinic phase.

The thermograms performed after crystallization toward the mesomorphic form (during cooling ramps performed with cooling rates in the range 100−160 K/s) up to about 70 °C closely follow the path of the thermograms performed after crystallizing toward the α-monoclinic phase (during cooling ramps performed with cooling rates in the range from 15 to 90 K/s); at 70 °C they deviate, and the deviation ends at about 130 °C, where again the thermograms performed after crystallization toward the mesomorphic form join those performed after crystallization toward the α-monoclinic phase. At high temperature they follow the same endothermic peak observed in the thermograms of the heating scans performed after solidification at cooling rates of 15 and 90 K/s.

The area between the two families of curves identifies an exothermal contribution, in the temperature interval 70−130 °C, which brings the enthalpy of the samples after crystallization toward the mesomorphic form down to the enthalpy of the samples crystallized in the α-monoclinic phase. This process can well be simply a chain reorganization process (melting−recrystallization) from the mesomorphic phase to the α-monoclinic phase. The net enthalpic effect accounts for the superposition of two large transitions with opposite signs occurring almost simultaneously, canceling each other's contributions (reorganization[34,41,45]), and appears small (about 20%) with respect to the area of the α melting peak. Obviously, as already observed by other authors[46,47] starting from a mesomorphic sample, the enthalpy increase related to the mesophase melting might be much larger than the net enthalpic effect seen between the curves.

The thermograms of the heating scans performed after cooling ramps carried out with cooling rates which did not allow crystallization neither toward the α-form nor completely toward the mesomorphic form (namely after cooling ramps carried out with cooling rates larger than 160 K/s) show an exothermic event, between 0 and 30 °C (center position at 7 °C), and at higher temperature they join all other thermograms and closely follow the path of the scans performed after cooling with cooling rates in the range 100−160 K/s, which had crystallized toward the mesomorphic phase. The exothermic event is consistent with a cold crystallization process to form the mesomorphic phase. The intensity (area) of crystallization peak increases with cooling rate applied during previous solidification; this is consistent with the observation that, during the corresponding cooling ramps, crystallization toward the α-monoclinic phase was not observed and the intensity of the crystallization peak toward the mesomorphic phase was found decreases (amorphization effect) on increasing cooling rate above 160 K/s.

The temperature of the mesomorphic crystallization peak corresponds to the low-temperature peak of the mesomorphic crystallization processes shown in Figure 5. This implies that at those temperatures the kinetic is already high enough to exhaust the crystallization process within about 10 K, which at the heating rate of 50 K/s adopted corresponds to a crystallization time of the order of 0.1 s; at higher heating rates the crystallization toward the mesomorphic form would have taken place at higher temperature.

The results of the analysis of phase distribution in samples obtained at high cooling rates (higher than 160 K/s) have to be considered on the basis of the findings reported above: even if cooling rate is such to prevent crystallization during the sample cooling, in the temperature interval 0−30 °C the kinetics of formation of the mesomorphic phase is such that during any type of analysis the equilibrium fraction of the mesomorphic phase would be reached. Therefore, calibration approaches of kinetic models on the basis of results of analysis of quenched samples should be reconsidered.

The exothermic low-temperature crystallization peak toward the mesomorphic phase was also observed by Caldas et al.[46] and Miyamoto et al.[48] upon heating quench cooled i-PP samples at heating rate of 20 and 10 K/min, respectively.

In both cases, the i-PP samples were prepared by melting a polymer film and then quenching into pentane at −160 °C. Miyamoto et al.[48] examined WAXS and SAXS intensities on heating of the quench-cooled samples. The WAXS intensity confirmed the crystallization toward mesophase starting from about −20 °C.

Furthermore, analyzing the thermogram of the heating of a quench-cooled sample in a pentane slush, reported by Caldas et al.,[46] it is possible to compare the heat of crystallization of exothermic peak, observed at low temperature, with the final heat of fusion of α-monoclinic phase. In the thermogram of Caldas et al.,[46] the ratio between the final heat of fusion (peak position at 160 °C) and the mesophase formation peak area at low temperature is about 8 (12.5%). This indicates substantial melting recrystallization during the heating scan, and that part of the crystallization enthalpy was not considered for peak integration or the sample prepared by Caldas et al. was not completely amorphous before the heating scan. The ratio between the same peak areas observed in this work, and reported in Figure 7, in the heating scan of the sample solidified at cooling rates of 1000 K/s is about 2.5 (40%), again indicating a melting recrystallization process probably in the temperature range 20−70 °C, which was not considered for peak integration.

The two observations together indicate that the sample prepared by Caldas et al. was not completely amorphous before the heating scan.

Furthermore, in the heating scan of the sample solidified at cooling rates of 1000 K/s, the sum of the crystallization peak of mesophase and the reorganization toward the α-phase is about 60% of the melting peak of the α-phase. Because of the uncertainty of the heat capacity measurement of about 20%, it is actually not possible to discuss these findings in a more quantitative way. This needs further improvement of the method, which is currently under way.

Conclusions

In this paper the thermograms of an i-PP at very high cooling and heating rates were obtained by a novel nanocalorimeter which can adopt samples having mass of the order of 100 ng and of about 10 μm thickness. Many cooling scans were carried out from 210 to −15 °C with cooling rates covering the range 15−1000 K/s; after each cooling scan the polymer was heated with heating rate of 50 K/s. The thermograms of the cooling ramps show that:

- Only the well-known α-monoclinic crystalline phase forms, when the i-PP is solidified at cooling rate up to about 90 K/s.
- At higher cooling rates (larger than 90 K/s), while the crystallization toward α-phase decreases, a second exothermic process starts to appear at low temperatures (below 40 °C). This process has to be related to the mesomorphic phase, which has been often observed in i-PP samples after solidification but never examined during crystallization.
- At even higher cooling rate (larger than 150 K/s), only the second low-temperature process takes place. These experimental results, summarized in crystallization peaks temperatures, give new phenomenological information about mesomorphic phase formation at high cooling rates.
- Furthermore, for cooling rates higher than 1000 K/s also the formation of the mesomorphic phase is prevented, and the sample stays amorphous.

The observed behaviors of cooling tests are confirmed and coherent with the behavior observed during subsequent heating runs which in addition show that:

- Samples, which could not crystallize in the α-form during cooling at high cooling rates, in the temperature interval 0−30 °C crystallize toward the mesomorphic phase within times of the order of 0.1 s.
- On heating at a rate of 50 K/s, the thermograms suggest that the mesomorphic phase could transform into the α-monoclinic phase in the interval 70−130 °C.

The cooling and heating ramps have given new important information, most of all with reference to temperature of mesophase formation. Nevertheless, these new information may be not easily used in order to define a crystallization kinetics of the mesophase. More direct and easy to interpret information may be obtained from isothermal tests after cooling the melt at a high cooling rate, with large enough undercooling.

Acknowledgment. Felice De Santis is grateful for a COST grant (COST-STSM-P12-00437). The main part of this work was carried out during a Short Term Scientific Mission (STSM) at Rostock University within the COST action P12 "Structuring of Polymers". This work was supported also by the Ministero dell'Istruzione, dell'Università e della Ricerca (PRIN 2004 titled "Control and Modeling of Morphology of Semicrystalline Polymers under Realistic Processing Conditions").

Supporting Information Available: A synoptic table of all the experiments and the figures showing all results of cooling scans and subsequent melting behaviors. This material is available free of charge via the Internet at http://pubs.acs.org.

References and Notes

(1) Addink, E. J.; Beintema, J. *Polymer* **1961**, *2*, 185−193.
(2) Vittoria, V. In *Handbook of Polymer Science and Technology*; Cheremisinoff, N. P., Ed.; Marcel Dekker: New York, 1989; Vol. 2, p 507.
(3) Brückner, S.; Meille, S. V.; Petraccone, V.; Pirozzi, B. *Prog. Polym. Sci.* **1991**, *16*, 361−404.
(4) Natta, G.; Peraldo, M.; Corradini, P. *Rend. Acad. Naz. Lincei* **1959**, *26*, 14−17.
(5) Miller, R. L. *Polymer* **1960**, *1*, 135−143.
(6) Glotin, M.; Rahalkar, R. R.; Hendra, P. J.; Cudby, M. E. A.; Willis, H. A. *Polymer* **1981**, *22*, 731−735.
(7) Corradini, P.; Petraccone, V.; De Rosa, C.; Guerra, G. *Macromolecules* **1986**, *19*, 2699−2703.
(8) Zannetti, R.; Celotti, G.; Fichera, A.; Francesconi, R. *Makromol. Chem.* **1969**, *128*, 137−142.
(9) Bassett, D. C.; Olley, R. H. *Polymer* **1984**, *25*, 935−943.
(10) Olley, R. H.; Bassett, D. C. *Polymer* **1989**, *30*, 399−409.
(11) Zhou, J.-J.; Liu, J.-G.; Yan, S.-K.; Dong, J.-Y.; Li, L.; Chan, C.-M.; Schultz, J. M. *Polymer* **2005**, *46*, 4077−4087.
(12) Hieber, C. A. *Polymer* **1995**, *36*, 1455−1467.
(13) Di Lorenzo, M. L.; Silvestre, C. *Prog. Polym. Sci.* **1999**, *24*, 917−950.
(14) Coccorullo, I.; Pantani, R.; Titomanlio, G. *Polymer* **2002**, *44*, 307−318.
(15) Di Lorenzo, M. L.; Silvestre, C. *Thermochim. Acta* **2003**, *396*, 67−73.
(16) Piccarolo, S.; Alessi, S.; Brucato, V.; Titomanlio, G. In *Crystallization of Polymers*; Dosière, M., Ed.; Kluwer Academic: Boston, 1993; p 475.
(17) Piccarolo, S. *J. Macromol. Sci., Phys. B* **1992**, *31*, 501−511.
(18) Strobl, G. *Eur. Phys. J. E* **2000**, *3*, 165−183.
(19) Lotz, B. *Eur. Phys. J. E* **2000**, *3*, 185−194.
(20) Cheng, S. Z. D.; Li, C. Y.; Zhu, L. *Eur. Phys. J. E* **2000**, *3*, 195−197.
(21) Muthukumar, M. *Eur. Phys. J. E* **2000**, *3*, 199−202.
(22) Pijpers, T. F. J.; Mathot, V. B. F.; Goderis, B.; Scherrenberg, R. L.; van der Vegte, E. W. *Macromolecules* **2002**, *35*, 3601−3613.
(23) Saunders, M.; Podluii, K.; Shergill, S.; Buckton, G.; Royall, P. *Int. J. Pharm.* **2004**, *274*, 35−40.
(24) Wu, Z. Q.; Dann, V. L.; Cheng, S. Z. D.; Wunderlich, B. *J. Therm. Anal.* **1988**, *34*, 105−114.
(25) Wilthan, B.; Cagran, C.; Pottlacher, G. *Int. J. Thermophys.* **2005**, *26*, 1017−1029.
(26) Lai, S. L.; Ramanath, G.; Allen, L. H.; Infante, P.; Ma, Z. *Appl. Phys. Lett.* **1995**, *67*, 1229−1231.
(27) Kwan, A. T.; Efremov, M. Yu.; Olson, E. A.; Schiettekatte, F.; Zhang, M.; Geil, P. H.; Allen, L. H. *J. Polym. Sci., Part B* **2001**, *39*, 1237−1245.
(28) Efremov, M. Yu.; Olson, E. A.; Zhang, M.; Lai, S.; Schiettekatte, F.; Zhang, Z. S.; Allen, L. H. *Thermochim. Acta* **2004**, *412*, 13−23.
(29) Efremov, M. Yu.; Olson, E. A.; Zhang, M.; Schiettekatte, F.; Zhang, Z. S.; Allen, L. H. *Rev. Sci. Instrum.* **2004**, *75*, 179−191.
(30) Adamovsky, S. A.; Minakov, A. A.; Schick, C. *Thermochim. Acta* **2003**, *403*, 55−63.
(31) Minakov, A. A.; Morikawa, J.; Hashimoto, T.; Huth, H.; Schick, C. *Meas. Sci. Technol.* **2006**, *17*, 199−207.
(32) Merzlyakov, M. *Thermochim. Acta*, in press.
(33) Adamovsky, S.; Schick, C. *Thermochim. Acta* **2004**, *415*, 1−7.
(34) Minakov, A. A.; Mordvintsev, D. A.; Schick, C. *Polymer* **2004**, *45*, 3755−3763.
(35) Minakov, A. A.; Mordvintsev, D. A.; Schick, C. *Faraday Discuss.* **2005**, *128*, 261−270.
(36) Gradys, A.; Sajkiewicz, P.; Minakov, A. A.; Adamovsky, S.; Schick, C.; Hashimoto, T.; Saijo, K. *Mater. Sci. Eng., A* **2005**, *413−414*, 442−446.
(37) Coppola, S.; Balzano, L.; Gioffredi, E.; Maffettone, P. L.; Grizzuti, N. *Polymer* **2004**, *45*, 3249−3256.
(38) Lamberti, G.; De Santis, F.; Brucato, V.; Titomanlio, G. *Appl. Phys. A* **2004**, *78*, 895−901.
(39) Pantani, R.; Speranza, V.; Coccorullo, I.; Titomanlio, G. *Macromol. Symp.* **2002**, *185*, 309−326.
(40) De Santis, F.; Ferrara, M.; Neitzert, H. C. *IEEE Trans. Instrum. Meas.* **2006**, *55*, 123−127.

(41) Minakov, A. A.; Adamovsky, S. A.; Schick, C. *Thermochim. Acta* **2005**, *432*, 177−185.
(42) TCG-3880 data sheet, Xensor Integration: http://www.xensor.nl/.
(43) van Herwaarden, A. W. *Thermochim. Acta* **2005**, *432*, 192−201.
(44) Brucato, V.; De Santis, F.; Giannattasio, A.; Lamberti, G.; Titomanlio, G. *Macromol. Symp.* **2002**, *185*, 181−196.
(45) Pyda, M.; Nowak-Pyda, E.; Heeg, J.; Huth, H.; Minakov, A. A.; Di Lorenzo, M. L.; Schick, C.; Wunderlich, B. *J. Polym. Sci., Part B: Polym. Phys.*, submitted for publication.
(46) Caldas, V.; Brown, G. R.; Nohr, R. S.; MacDonald, J. G.; Raboin, L. E. *Polymer* **1994**, *35*, 899−907.
(47) Wang, Z.-G.; Hsiao, B. S.; Srinivas, S.; Brown, G. M.; Tsou, A. H.; Cheng, S. Z. D.; Stein, R. S. *Polymer* **2001**, *42*, 7561−7566.
(48) Miyamoto, Y.; Fukao, K.; Yoshida, T.; Tsurutani, N.; Miyaji, H. *J. Phys. Soc. Jpn.* **2000**, *69*, 1735−1740.

MA052525N